Journal of Biomaterials and Nanobiotechnology, 2018, 9, 277-289
http://www.scirp.org/journal/jbnb
ISSN Online: 2158-7043
ISSN Print: 2158-7027

Synthetic Three-Dimensional Scaffold for Application in the Regeneration of Bone Tissue

Dante Jesus Coletta[1#], Liliana Raquel Missana[2#], Talita Martins[3#], Maria Victoria Jammal[2], Luciano Andrés García[1], Nayla Farez[1], Tomas De Glee[1], João Paulo Mardegan Issa[4], Sara Feldman[1*]

[1]LABOATEM, Medicine School, Rosario National University, Rosario, Argentine
[2]Oral Pathology Department, Dental School, Experimental Pathology Laboratory, National University—PROIMI-CONICET, Tucuman, Argentine
[3]Biomaterials Laboratory, Minas Gerais Federal University, Belo Horizonte, Brazil
[4]School of Dentistry of Ribeirão Preto, University of São Paulo, Ribeirão Preto, São Paulo, Brazil
Email: *saryfeldman@gmail.com

How to cite this paper: Coletta, D.J., Missana, L.R., Martins, T., Jammal, M.V., García, L.A., Farez, N., De Glee, T., Issa, J.P.M. and Feldman, S. (2018) Synthetic Three-Dimensional Scaffold for Application in the Regeneration of Bone Tissue. *Journal of Biomaterials and Nanobiotechnology*, **9**, 277-289.
https://doi.org/10.4236/jbnb.2018.94016

Received: July 13, 2018
Accepted: September 8, 2018
Published: September 11, 2018

Abstract

Bone tissue engineering aims to use biodegrade able scaffolds to replace damaged tissue. This scaffold must be gradually degraded and replaced by tissue as similar as possible to the original one. In this work a hybrid porous scaffold containing chitosan, polyvinyl alcohol and bioactive glass was successfully obtained and subsequently characterized by scanning electron microscopy. The scaffold presented satisfactory pore size range and open interconnected pores, which are essential for tissue ingrowth. A cytotoxicity assay showed that this biomaterial allows adequate cell viability, so that it was considered suitable for an *in vivo* experiment. Promising results were obtained with the implant of the scaffold in an experimental model of a New Zealand rabbit femur bone lesion. Clinical and biochemical parameters measured such as complete blood count, total serum proteins, albumin, alanine aminotransferase and aspartate aminotransferase were similar between animals in the control group at all time periods studied. Histological and histometric studies showed that the scaffold was coated with a cement-like substance, exhibiting many areas of mineralized structures. Very few osteocyte-like cells or lining-like cells were found inside the amorphous mineralized deposit. *In vivo* results allow us to consider this scaffold as a promising biomaterial to be applied in bone tissue engineering.

Keywords

Biomaterial Scaffold, Bone, Chitosan, Poly(Vinyl Alcohol-Co-Vinyl Acetate)

[#]These authors contributed equally to this work.

1. Introduction

Synthetic three-dimensional scaffolds for application to the regeneration of bone tissue should present an architecture similar to bone extracellular matrix and provide a suitable microenvironment for cell adhesion, proliferation and differentiation, ensuring tissue growth [1] [2]. Among other properties, these scaffolds should exhibit biocompatibility with the damaged tissue, interconnected pore network, pore size ranging from 100 to 300 μm, mechanical strength similar to bone tissue, and biodegradability at the rate at which tissue regenerates [3] [4].

Chitosan (Chi) can be considered as one of the most thoroughly investigated materials in recent years. The non-toxicity, high biocompatibility, and antigenicity of chitosan have driven its potential applications in biomedical field [5] [6] [7]. The biodegradability of chitosan favors its use as a biomaterial in tissue engineering and drug delivery systems. One aspect of this polymer that limits its application is its brittleness. Moreover, for tissue engineering applications, it is important to have a predictable kinetics of the biodegradability of the polymer. One way to obtain the desired properties is the use of natural or synthetic polymers, either alone or blended, with grafted or crosslinked networks [7] [8] [9] [10].

In other words, the polymer blend and cross-linked polymer system may present a different degradation behavior under physiological fluid conditions, where part of the polymer network may undergo fast solvation and another portion may experience slow degradation by depolymerization. Hence, chitosan joined to other polymers has opened a new line of research for altering or tailoring the property of interest. In previous works [11] [12], the approach used for modulating degradability and flexibility of the polymer was by blending chitosan with poly(vinyl alcohol-co-vinyl acetate) (Chi/PVA blend), followed by chemical crosslinking with glutaraldehyde (GA).

Mechanical strength of porous scaffolds are also crucial with respect to the regeneration of hard tissue such as bone, which must support a load and meet specific mechanical needs while stimulating bone regeneration. The most investigated approach to attain the desired levels of strength is the production of composites and hybrid systems [13] [14] [15] [16] in which a bioceramic phase is added to the degradable polymer matrix as a reinforcing agent. Bioactive glasses in the system SiO_2-CaO-P_2O_5 have been largely investigated as bioactive ceramics to be introduced into the organic phase due to their osteoconductive and osteoinductive properties [17] [18].

In previous works [19] [20], hybrid porous scaffolds containing chitosan, PVA and bioactive glass were successfully obtained via a lyophilization method. Ch/PVA hybrids with 20% bioactive glass (w/w) cross-linked with glutaraldehyde showed adequate pore structure and relatively low mass loss during an *in vitro* degradation test, with preservation of their physical macroscopic structure, which are suitable characteristics for application in tissue engineering.

We developed a model of bone lesion in a New Zealand rabbit femur, which does not resolve spontaneously, with the generation of a fibrous tissue that does not have the original characteristics of the tissue prior to the injury, in order to use it to consider the osteoregenerative potential characteristic of the scaffolds to be tested [21] [22] [23].

The present work investigates Ch/PVA containing 20% of bioactive glass (w/w), with a Ch:PVA mass ratio of 1:1. Pore size, morphological and *in vitro* cytotoxicity characteristics were evaluated to characterize these biomaterials. We also tested the biomaterial in an *in vivo* implant procedure in our experimetal model of New Zealand rabbit femur bone lesion, considering not only the implant tissues but also the post-surgical clinical and biochemical studies of the animals.

2. Method

2.1. Preparation of Polymer and Bioactive Glass Precursor Solutions

All reagents were supplied by Aldrich Chemical. Poly(vinyl alcohol) (PVA) solution 5.0% (w/v) was prepared by dissolving PVA (80% hydrolysis) in deionized water (100 mL) under mechanical stirring speed of 280rpm at 70˚C (±2˚C) for 45 minutes.

A solution of Chitosan (C) with high molecular weight and deacetylation (DD) > 75% (1% w/v) was prepared by dissolving 1 g commercial powder in 100 ml deionized water. 2 ml acetic acid was added to the solution, and then subjected to mechanical stirring for 24 hours. Bioactive glass 60 s precursor solution (BG) was obtained by acid hydrolysis and polycondensation of Tetraethylorthosilicate (TEOS-($Si(OC_2H_5)_4$)), alkoxide precursor of SiO_2, and Triethylphosphate (TEP-($(C_2H_5O)_3PO$)), alkoxide precursor P_2O_5. Hydrolysis occurred by adding deionized water and nitric acid as catalyst reagents. 85 g of Calcium Nitrate ($Ca(NO_3)_2{\cdot}4H_2O$) was then added as a precursor of CaO. The nominal composition of the bioactive glass was the following: 60% SiO_2, 36% CaO; 4% P_2O_5. Glutaraldehyde solution (2.0% w/v) was prepared by diluting 25% glutaraldehyde 2 ml in 23 ml deionized water.

2.2. Scaffolds Production (SBG, Scaffolds of Bioactive Glass)

The scaffolds were fabricated by mixing PVA solution with Chitosan solution with a CHI to PVA ratio of 1:1, as shown in Table 1, and mixing under agitation for 30 minutes at room temperature. The precursor solution of bioactive glass (20% of the total weight of the scaffold) was added and mechanical stirring was continued for 45 minutes. Finally, the 2% glutaraldehyde solution (3% polymer mass) was added and mechanical stirring continued for 15 minutes, as shown in Table 1.

The resulting solution was poured into 7 ml vials with a syringe and kept at room temperature for 72 hours, the time required for gelation to occur. The vials

Table 1. Composition of scaffold.

Scaffold CHI:PVA ratio	Composition (%)			
	Chitosan	PVA	VB	Glutaraldehyde*
1:1	40	40	20	3

*In relation to polymers mass.

were kept tightly closed during gelation and then frozen for 72 hours in a refrigerator at −20˚C. The frozen vials were immersed in liquid nitrogen for 20 minutes and then placed in the lyophilizer (Model: K105-Company Liotop-SP/Brazil) for 48 h with −98˚C condenser temperature and −4˚C sample collector temperature. The pressure in the collector was 30 mmHg.

2.3. Structural Characterization of Three-Dimensional SGB

Scanning Electron Microscopy (SEM) FEI-Inspect-S50/Czech Republic was used for scaffold characterization. Previously, samples were frozen by liquid nitrogen immersion and fractured in order to obtain the internal fracture surface for analysis. This surface was coated with gold.

2.4. Cytotoxicity Assay

The cyxotoxicity assay aims to detect the potential of a material or device to produce lethal or sublethal effects on biological systems at the cell level. The release of toxic subproducts of the biomaterial can damage the cells or reduce the rate of cell culture growth. A biomaterial can be considered toxic for use in a biological system when it shows under 50% of cell viability compared to the positive control. Formazan crystals were solubilized and optical density was determined by a spectrophotometer at 595 nm. Primary culture of human fibroblasts at the fourth passage was plated in 24-well plates at a density of 1×10^4 cells/well. Cell populations were normalized with DMEM for 24 hours, after which time the medium was changed and the samples were placed into wells. The cylindrical samples were sliced into four equal parts, sterilized by irradiation at 15 kGy for 30 minutes, and then soaked in saline solution (PBS) for 24 hours. DMEM was used as an experiment positive control and PBS 10× as a negative control. All assays were performed in triplicate (n = 3). Cells were incubated at 37˚C in a 5% CO_2 humidified atmosphere for 72 hours. At the end of the incubation period, the culture medium was removed and discarded and 210 µL/well of DMEM was added. Then 170 µL/well of MTT solution (Invitrogen) (5 mg/ml) was added and the plate was incubated at 37˚C in a 5% CO_2 humidified atmosphere for 2 hours. The cells were observed under an optical microscope (MO) to display the formazan crystals that were solubilized by the addition of 210 µL/well of a solution of SDS 10%-HCl (0.01 M hydrochloric acid—10% of sodium dodecyl sulfate water) followed by incubation at 37˚C in a 5% CO_2 humidified atmosphere for 18 hours. 100 µL was transferred from each well to a 96-well plate, in triplicate, and optical density was measured in a spectrophotometer at 595 nm. All the

steps were performed in minimuml lighting conditions. Results were analyzed using one-way ANOVA test followed by Bonferroni test and expressed as mean ± SEM.

2.5. *In Vivo* Experiments

2.5.1. Experimental Units

Adult female New Zealand white rabbits with an average weight of 3.5 kg (n = T10) were randomly divided into two groups: C (Control) and T (treated rabbits with bone defects caused by surgery). Rabbits were kept in individual cages with food (PROVIFE, Argentina) and water *ad libitum*. Experimental procedures regarding the use of animals were approved by the Bioethics Committee of Rosario National University (Resolution No. 150/2015). Its regulations are in agreement with the well-established guidelines for animal care and manipulation to decrease pain and suffering of the animal, according to the 3Rs (replacement, reduction and refinement) and follow international laws for the care and use of laboratory animals.

2.5.2. Pre-Surgical Preparation

Antibiotic prophylaxis and anesthetic treatment were performed according to a procedure previously described [23]. Prior to the surgical procedure, rabbits received antibiotic prophylaxis (cefazolin at a dose of 50 mg/kg/day, intramuscularly administered). The anesthetic treatment was performed by combining three drugs intramuscularly administered: Ketamine Hydrochloride at 35 mg/kg/day, Xylazine Hydrochloride (2.0%) at 18 mg/kg, and Acepromazine Maleate (1.0%) at 1 mg/kg, achieving complete relaxation of the animal. The anesthetic effect lasted 45 - 60 minutes.

2.5.3. Surgical Procedure

Surgical techniques were performed in a similar way to a procedure previously described (38). The intervention began with a longitudinal cutaneous incision of 4 cm in the internal lateral distal metaphysis of the femur, immediately above the medial condyle. Medial and lateral flaps were divided, and a non-muscular aponeurotic plane was opened until reaching the desired bone area. The central point of the perforation was marked with a bradawl, and a 6 mm diameter lesion was made using a drill attached to a sterile (UV) electric motor. The hemostasis of the lesion was performed using a sterile swab plus gauze. Then, the area was dried with a sterile gauze. The tested scaffolds, SGB, previously rehydrated in the animal`s own blood, were implanted and the wounds were sutured. The aponeurotic plane was first sutured using resorbable material type 3/0; the skin was sutured with 3/0 Nylon and disinfected with povidone-iodine.

2.5.4. Post-Surgical Clinical Studies

During the study period, animals were clinically monitored on a daily basis as to overall status, mobility and food intake. Body temperature was measured daily during the first week, and then weekly. Biochemical parameters were evaluated

by standard procedures at days 0, 2, 30 and at the end of the study; complete blood count, total serum proteins, albumin, alanine aminotransferase (ALT) and aspartate aminotransferase (AST) were evaluated by standard procedures commercial kits (Wiener lab Group, Argentina). The results were compared to the results obtained from control animals of the same age at each time period and analyzed using the Kruskall-Wallis test.

2.5.5. Animal Euthanasia and Sample Collection

Three months after surgery, animals were euthanized using three doses of anaesthesia, as previously described for other experimental models [24]. Then, femurs were collected for use in different experiments aimed at assessing bone regeneration (see below).

3. Histological Studies

Distal epiphysis from femurs were obtained after cuts made 4 cm above the metaphysis with a carborundum disc cutter (Dochem, China) using a dental drill under irrigation with distilled water. The implanted matrix areas were marked with Indian ink. The samples were subjected to decalcification using modified Morse solution (Okayama University Dental School) and embedded in paraffin following well-established protocols. Then samples were serially cut (5 μm) to obtain oriented tissues (ephiphysis, metaphysis with implanted matrix on the same plane) and stained with Hematoxylin & Eosin (H&E) and Masson's Trichromic. All specimens were examined with light microscopy and evaluated by a single pathologist. Subsequently, another pathologist (certified by the Health Ministry of Argentina. license N˚ 31455) performed an independent review to verify microscopic observations. The reported results reflect the mutually-agreed-upon diagnoses by both pathologists. Photomicrographs were taken from slides of each specimen by means of an Olympus SC50 camera adapted to Olympus BX 43 microscope using CellSens Standard 1.17 Olympus Soft 2009-2017 and Olympus stereo zoom SZ 51.

Histometric Analysis: Photomicrographs were taken from slides of each specimen, with an Olympus SC50 camera adapted to an Olympus BX 43 microscope using CellSens Standard 1.17 Olympus Soft 2009-2017. Five photos of each slide from the hybrid matrix area at 40× magnification, were obtained. The compartments chosen were: cement mineralized substance, inflammatory infiltrate and interstitial tissue measured with Image Pro Plus analysis system (Media Cybernetics, Silver Spring, MD, USA Version 4.5.0.29 for Windows 1998/NT/2000). Values were expressed as percentages [25].

4. Results

4.1. Structural Characteristics of Three-Dimensional Scaffolds

The SGB pore morphology was analyzed by SEM and is shown in **Figure 1**, which shows a network of well-defined, open and interconnected pores with thin walls. Homogeneous and organized porosity was observed, pore size in the

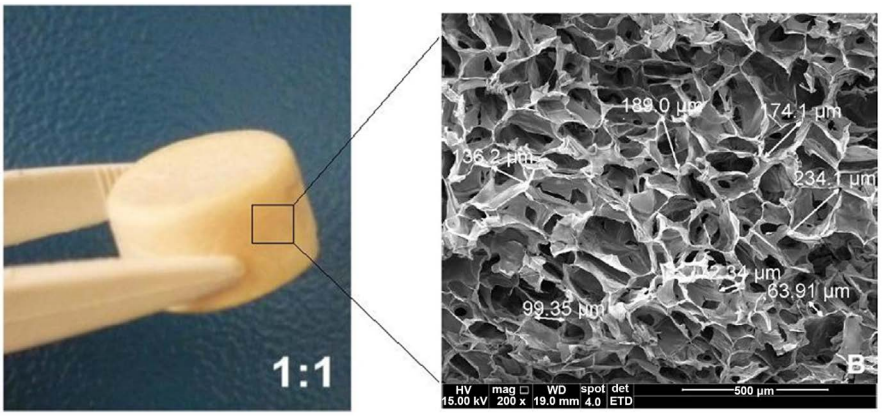

Figure 1. Structural characteristics of three-dimensional scaffold by scanning electron microscopy (SEM).

regions analyzed ranging from 64 to 234 µm in 1:1 scaffold. The scaffolds presented satisfactory pore size range, and opened interconnected pores, which are essential for tissue ingrowth. The presence of pores of different sizes is very important since bone tissue grows through interconnected pores in the range from 100 to 200 µm, while cell adhesion and vascular formation occur with pores whose size is smaller than 100 µm.

4.2. Cytotoxicity

The cells cultures directly in the presence of 1:1 scaffold presented above 90% viability. The assay showed that this biomaterial allows adequate cell viability and is considered suitable for *in vivo* tests (**Figure 2**).

4.3. Clinical and Biochemical Results

The welfare of the animals during the first two days post-implantation was slightly affected, with disrupted walking, as expected. After six days, treated animals behaved similarly to their non-operated control counterparts. Temperature values, food intake and all biochemical parameters measured in the treated group were similar between control animals at every time studied (n.s.d., $p > 0.05$).

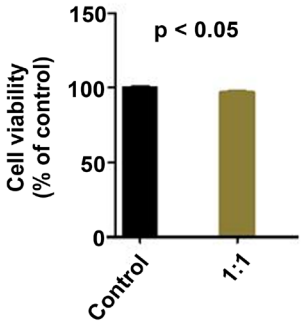

Figure 2. Cell viability for scaffolds 1:1 compared to negative control.

4.4. Histological Results (Figure 3: Photos 3(a), 3(b), 3(c), 3(d), 3(e), 3(f))

Two areas were selected to evaluate *in vivo* bone biocompatibility: 1) Femur-scaffold interface experimental lesion, and 2) Scaffold.

1) A bi-layer tissue was observed at the femur-scaffold interface formed by an inner thick fibrous tissue surrounded by an outer thick bone layer (Photo 3(a)). The new bone layer was formed by lamellar and reticular trabecular bone, thus forming the composite bone and located in the FEL (femoral experimental lesion). Close to this area, few hematopoietic tissue spaces were distinguished (Photo 3(b)). Micro-haemorrhage areas and micro-fragmented foreign body particles similar to SBG surrounded by dilated congestive blood vessels were observed.

2) Scaffold

The SGB surface was coated with a cement-like mineralized substance, osteoblast-like cells were attached and extracellular matrix was produced (Photo 3(c)), and newly formed bone anchored on the SGB surface (Photo 3(d)). Inside the new bone tissue formation, some bone particles probably obtained from the surgery process were found (Photo 3(e)). They were surface resorbed and covered by new bone formation; scattered osteogenesis was initiated inside them. Very few osteocyte-like cells and lining-like cells were found inside the amorphous mineralized deposit. Also, erythrocytes, lymphocytes and macrophages as well as cells debris were observed inside the scaffold (Photo 3(f)).

4.5. Histometric Results

Inside the SGB matrix, 64% bone-cement mineralized substance and 28% inflammatory exudate were produced, with 8% interstitial space (**Table 2**).

5. Discussion

The amount of mechanical stimulation performed by the scaffold depends on the porosity, pore size, pore distribution, architecture and mechanical properties of the materials. The presence of pores of different sizes is very important since bone tissue grows through interconnected pores in the range between 100 and 200 μm, while cell adhesion and vascular formation occur in pores below 100 μm. The presence of macropores (>100 μm and <500 μm) is ideal for the growth and adhesion of the cells and the release of the nutrients to the center of the newly forming tissue. The ideal pore size for the growth of bone tissue is between 75 and 250 μm [26].

A biomaterial can be considered toxic for use in biological systems when it causes under 50% of cell viability. The assay conducted in this study showed that this biomaterial allows adequate cell viability and is considered suitable for *in vivo* testing.

The implantation of SGB did not cause either clinical or biochemical alterations in the implanted animals, which is promising for future considerations of implants in other types of injuries. Certain scaffolds, when degraded, produce

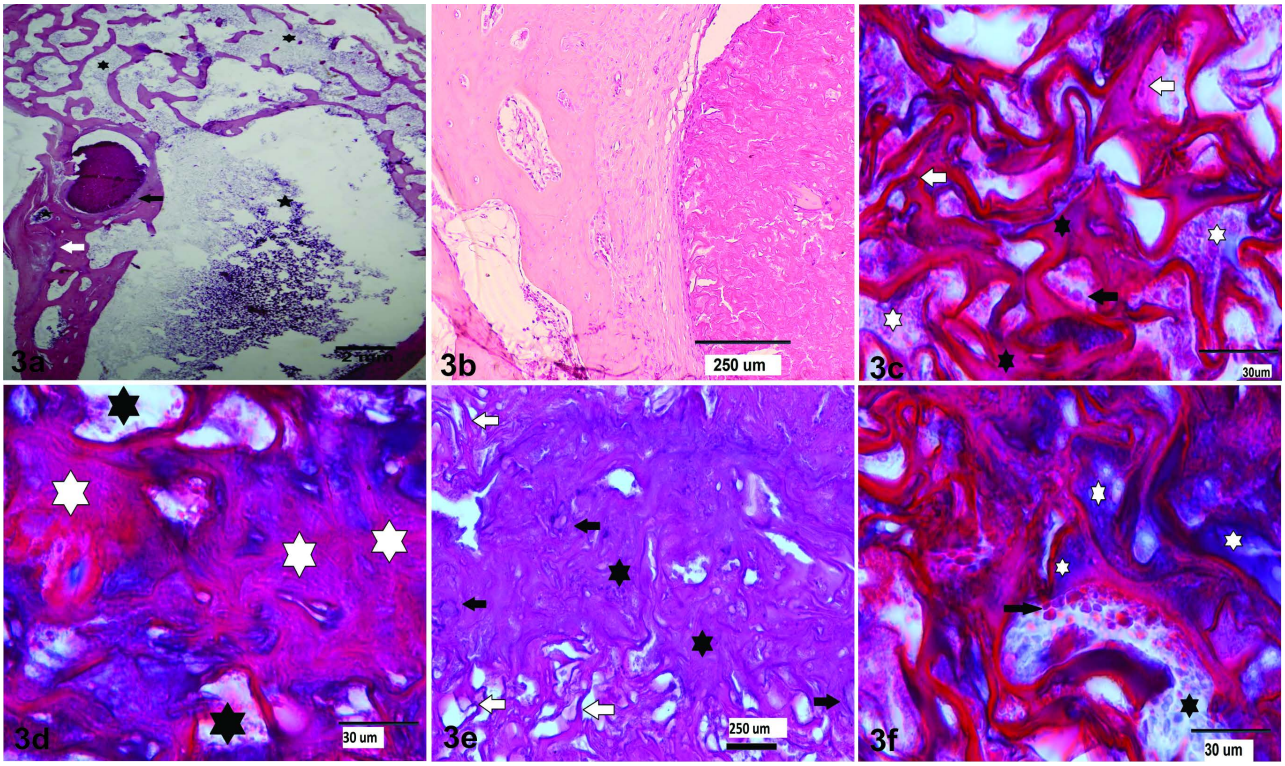

Figure 3. (a) Low magnification photomicrograph showing the scaffold-interface (1:1), a bi-layer of fibrous and bone tissues. They were similar to a discontinued double capsule (black arrow). New compound bone was deposited into the FEL (femoral experimental lesion) (white arrow). Inside the new bone, few hematopoietic tissue spaces showing micro-haemorrhages (black asterisk) were observed. H&E stained. Magnification 7.35×, Bar = 2 mm; (b) Photomicrograph from the Experimental Group showing hematopoietic bone marrow (white arrow) between trabeculae (black asterisk) surrounded by extended branches of blood vessels congestive and micro-haemorrhages (black arrow). H&E stained. Magnification 116.7×, Bar = 250 μm; (c) Photomicrograph showing inside and over SGB extended areas of cement mineralized substance formation (black asterisks) with few osteocyte-like cells (white arrow) inside and lined by osteoblast-like cells (black arrow). Macrophages, cells and material debris were observed (white asterisks). Masson's Trichromic staining. Magnification 1000×, Bar = 30 μm; (d) Photomicrograph showing extended bone-like formation area (white asterisks) inside SGB. In the scaffold spaces, inflammatory cells and particles debris were found (black asterisks). Masson's Trichromic staining. Magnification 1000×, Bar = 30 μm; (e) Photomicrograph inside SGB showing bone particles left from surgery, basophilic lined (black arrows) surrounded by newly formed bone (black asterisk). Outside, cement mineralized substance was found on SGB (white arrows). H&E stained. Magnification 400×, Bar = 500 μm. (f) Photomicrograph from implanted SGB showing cement mineralized substance deposited on matrix surface, outlined by bone-like extracellular matrix lined by osteoblast-like cells (black arrow), and spaces with inflammatory cells and rest debris (black asterisk). Masson's Trichromic staining. Magnification 1000×, Bar = 30 μm.

Table 2. Histometric results.

total area	Percentage of
Cement Mineralized Substance	64
Inflammatory Exudate	28
Interstitial Space	8

undesirable secondary effects at the metabolic level or generate hepatic alterations. The fact that SGB implants did not produce any detectable alterations indicates that they are biocompatible.

Our results showed that SGB underwent fast degradation and size decrease after bone implantation at FEL (femoral experimental lesion, thus showing its ability to be resorbed. Inside SGB, 64% of cement mineralized substance, similar to hydroxy carbonate apatite-like (HCA) reaction layer, was produced on its surface, covered by new bone-like formation with few osteocyte-like cells inside and lining-like cells outside, after implantation into the host tissues, as a result of bioactive glass component reaction [27].

Moreover, the cement mineralized substance showed a granulated aspect that could be explained by dissolution, leaching and precipitation of SGB [28].

The presence of 28% inflammatory cells and macrophages found in our results could be explained by Vander *et al.* [29] and Rodriguez Vazquez *et al.* [30], who claimed that chitosan in the manufactured scaffold and its oligomers stimulated macrophages activity, increasing nitric oxide, IL1 and TNF α as well as TGF β and PDGF. Moreover, they asserted that chitosan is hypoallergenic and only transiently stimulated the immune system because it was metabolized. Spieller *et al.* [31], in *in vitro* and *in vivo* studies that differed from traditional paradigms, found evidence that all three macrophage phenotypes (M1, M2a and M2c) support angiogenesis in different ways. M1 and M2c macrophages induced endothelial cell sprouting, while M2a macrophages promoted anastomosis. By modifying scaffold properties to control macrophage response, we were able to achieve better vascularization and manipulate bone formation.

It could be considered that the lower values from macrophages allowed us to observe bone-like formation as well as osseointegration inside the scaffold of bone particles from the host bone, detached throught the experimental surgery lesion. This concept was supported by Li *et al.* [32] who demonstrated that an HCA layer obtained from bioactive glass was crucial and needed to be formed without being disturbed at the implant-tissue interface at the appropriate time to match the repair rate steps in the healing sequence of the implant site. With respect to the interactions between the biomaterial and the host tissues, our results showed a cement-like deposit of amorphous calcium phosphate phase deposits, crystallizing to hydroxyapatite (HA), bonded to collagen fibrils produced by osteoblasts on the scaffold surface. At the scaffold-tissue interface, a thick double fibrous-bony capsule was formed. Nagai *et al.* [33] demonstrated that there are four types of implant-tissue response: a) If the material is toxic, the surrounding tissues die; b) If the material is nontoxic and biologically inactive (nearly inert), a fibrous tissue of variable thickness is formed; c) If the material is nontoxic and biologically bioactive, an interface bond is formed and d) If the material is nontoxic and dissolves, the surrounding tissue replaces it. In this context, we consider that our SGB interactions response with the tissue could be evaluated as c), because inside bone formation was deposited on the scaffold.

6. Conclusion

The scaffold obtained through the lyophilization route showed adequate pore

structure, presenting high porosity and suitable interconnected pores. The biological test provides evidence that it was non-toxic for the cell culture, which confirms that the biomaterials were adequate for the subsequent *in vivo* test. *In vivo* results allow us to consider SGB scaffold as a promising bone tissue engineering biomaterial.

Conflicts of Interest

The authors declare no conflicts of interest regarding the publication of this paper.

References

[1] Amini, A., Laurencin, C.T. and Nukavarapu, S.P. (2012) Bone Tissue Engineering: Recent Advances and Challenges. *Critical Reviews™ in Biomedical Engineering*, **40**, 363-408. https://doi.org/10.1615/CritRevBiomedEng.v40.i5.10

[2] Zohora, F.T. and Azim, A.Y. (2014) Biomaterials as Porous Scaffolds for Tissue Engineering Applications: A Review. *European Scientific Journal*, **10**, 186-209.

[3] Cheung, H.Y., Lau, K.T., Lu, P.T. and Hui, D.A. (2007) Critical Review on Polymer-Based Bio-Engineered Materials for Scaffold Development. *Composites Part B: Engineering*, **38**, 291-300. https://doi.org/10.1016/j.compositesb.2006.06.014

[4] Petrovic, V., Zivkovic, P., Petrovic, D. and Stefanovic, V. (2012) Craniofacial Bone Tissue Engineering. *Oral Surgery*, *Oral Medicine*, *Oral Pathology*, *Oral Radiology*, **114**, e1-e9, https://doi.org/10.1016/j.oooo.2012.02.030

[5] Zargar, V., Asghari, M. and Dasht, A. (2015) A Review on Chitin and Chitosan Polymers: Structure, Chemistry, Solubility, Derivatives, and Applications. *Chemical Biological Engineering Reviews*, **2**, 204-226.

[6] Liu, Y.L., Su, Y.H. and Lai, J.Y. (2004) *In Situ* Crosslinking of Chitosan and Formation of Chitosan-Silica Hybrid Membranes with Using γ-Glycidoxypropyltrimethoxysilane as a Crosslinking Agent. *Polymer*, **45**, 6831-6837.

[7] Subramanian, A., Rau, A.V. and Kaligotla, H. (2006) Surface Modification of Chitosan for Selective Surface-Protein Interaction. *Carbohydrate Polymers*, **66**, 321-332. https://doi.org/10.1016/j.carbpol.2006.03.022

[8] Hennink, W.E. and van Nostrum, C.F. (2002) Novel Crosslinking Methods to Design Hydrogels. *Advanced Drug Delivery Reviews*, **54**, 13-36. https://doi.org/10.1016/S0169-409X(01)00240-X

[9] Ma, L., Gao, C., Mao, Z., Zhou, J., Shen, J., Hu, X. and Han, C. (2003) Collagen/Chitosan Porous Scaffolds with Improved Biostability for Skin Tissue Engineering. *Biomaterials*, **24**, 4833-4841. https://doi.org/10.1016/S0142-9612(03)00374-0

[10] Mansur, H.S. and Costa, H.S. (2008) Nanostructured Poly(Vinyl Alcohol)/Bioactive Glass and Poly(Vinyl Alcohol)/Chitosan/Bioactive Glass Hybrid Scaffolds for Biomedical Applications. *Chemical Engineering Journal*, **137**, 72-83. https://doi.org/10.1016/j.cej.2007.09.036

[11] Costa-Junior, E.S. and Mansur, H.S. (2008) Preparation and Characterization of Chitosan/Poly(Vinyl Alcohol) Blends Chemically Crosslinked with Glutaraldehyde for Application in Tissue Engineering. *Química Nova*, **31**, 1460-1466.

[12] Costa-Junior, E.S., Pereira, M.M. and Mansur, H.S. (2009) Properties and Biocompatibility of Chitosan Films Modified by Blending with PVA and Chemically Cros-

slinked. *Journal of Materials Science*: *Materials in Medicine*, **20**, 553-561. https://doi.org/10.1007/s10856-008-3627-7

[13] Pereira, M.M., Jones, J.R., Orefice, R.L. and Hench, L.L. (2005) Preparation of Bioactive Glass-Polyvinyl Alcohol Hybrid Foams by the Sol-Gel Method. *Journal of Materials Science*: *Materials in Medicine*, **16**, 1045-1050. https://doi.org/10.1007/s10856-005-4758-8

[14] Rezwan, K., Chen, Q.Z., Blaker, J.J. and Boccaccini, A.B. (2006) Biodegradable and Bioactive Porous Polymer/Inorganic Composite Scaffolds for Bone Tissue Engineering. *Biomaterials*, **27**, 3413-3431. https://doi.org/10.1016/j.biomaterials.2006.01.039

[15] Wang, Y., Yang, C.X., Chen, X. and Zhao, N. (2006) Development and Characterization of Novel Biomimetic Composite Scaffolds Based on Bioglass-Collagen-Hyaluronic Acid-Phosphatidylserine for Tissue Engineering Applications. *Macromolecular Materials and Engineering*, **291**, 254-262. https://doi.org/10.1002/mame.200500381

[16] Rodrigues, C.V.M., Serricella, P. and Linhares, A.B.R. (2003) Characterization of a Bovine Collagen-Hydroxyapatite Composite Scaffold for Bone Tissue Engineering. *Biomaterials*, **24**, 4987-4997. https://doi.org/10.1016/S0142-9612(03)00410-1

[17] Jones, J.R. (2015) Review of Bioactive Glass: From Hench to Hybrids. *Acta Biomater*, **23**, S53-S82. https://doi.org/10.1016/j.actbio.2015.07.019

[18] Rahaman, M.N., Day, D.E., Sonny, B.B., Fu, Q., Jung, S.B. and Bonewald, L.F. (2011) Bioactive Glass in Tissue Engineering. *Acta Biomater*, **7**, 2355-2373. https://doi.org/10.1016/j.actbio.2011.03.016

[19] Elke, M.F., Lemos, P.S.O. and Pererira, M.M. (2016) 3D Nanocomposite Chitosan/Bioactive Glass Scaffolds Obtained Using Two Different Routes: An Evaluation of the Porous Structure and Mechanical Properties. *Química Nova*, **39**, 462-466.

[20] Silva, A.P.R., Macedo, T.L., Coletta, D.J., Feldman, S. and Pereira, M.M. (2016) Synthesis, Characterization and Cytotoxicity of Chitosan/Polyvinyl Al-Cohol/Bioactive Glass Hybrid Scaffolds Obtained by Lyophilization. *Matéria*, **21**, 964-973. https://doi.org/10.1590/s1517-707620160004.0089

[21] Coletta, D.J., Ibañez-Fonseca, A., Missana, L., Jamma, L.M.V., Vitelli, E., Aimone, M., Zabalza, F., Issa. J., Rodriguez-Cabello, J.C. and Feldman, S. (2017) Bone Regeneration Mediated by a Bioactive and Biodegradable ECM.Like Hidrogel Base Don elastin-Like Recobinamers. *Tissue Engineering Part A*, **23**, 1361-1371. https://doi.org/10.1089/ten.tea.2017.0047

[22] Coletta, D.J., Lozano, D., Rocha-Oliveira, A.A., Mortarino, P., Bumaguin, G.E., Vitelli, E., Vena, R., Missana, L., Jammal, M.V., Portal-Núñez, S., Pereira, M., Esbrit P. and Feldman, S. (2014) Characterization of Hybrid Bioactive Glass-Polyvinyl Alcohol Scaffolds Containing a PTHrP-Derived Pentapeptide as Implants for Tissue Engineering Applications. *Open Biomedical Engineering Journal*, **8**, 20-27. https://doi.org/10.2174/1874120701408010020

[23] Goy, D.P., Gorosito, E., Costa, H.S., Mortarino, P., Pedemonte, N.A., Toledo, J. and Feldman, S. (2012) Hybrid Matrix Grafts to Favor Tissue Regeneration in Rabbit Femur Bone Lesions. *Open Biomedical Engineering Journal*, **6**, 85-91.

[24] Feldman, S., Cointry, G.R., Leite Duarte, M.E., Sarrió, L., Ferretti, J.L. and Capozza, R.F. (2004) Effects of Hypophysectomy and Recombinant Human Growth Hormone on Material and Geometric Properties and the Pre- and Post-Yield Behavior of Femurs in Young Rats. *Bone*, **34**, 203-215. https://doi.org/10.1016/j.bone.2003.09.006

[25] Weibel, E.R., Kistler, G.S. and Scherle, W.F. (1966) Practical Stereological Methods

for Morphometric Cytology. *Journal of Cell Biology*, **30**, 23-28. https://doi.org/10.1083/jcb.30.1.23

[26] Sabree, I., Gough, J.E. and Derby, B. (2015) Mechanical Properties of Porous Ceramic Scaffolds: Influence of Internal Dimensions. *Ceramics International*, **41**, 8425-8432. https://doi.org/10.1016/j.ceramint.2015.03.044

[27] Filgueiras, R.M. and Hench, L.L. (1993) Solution Effects on the Surface Reactions of a Bioactive Glass. *Journal of Biomedical Materials Research*, **27**, 445-453. https://doi.org/10.1002/jbm.820270405

[28] West, J.K. and Hench, L.L. (1994) AM-1 Molecular Orbital Calculations of Silica-Alanine-Nitrogen Interaction. *Journal of Biomedical Materials Research*, **28**, 625-633. https://doi.org/10.1002/jbm.820280513

[29] VandeVord, P., Mattehewn, H., DeSilva, S., Mayton, L., Wu, B. and Wooley, P. (2002) Evaluation of the Biocompatibility of the Chitosan Scaffold in Mice. *Journal of Biomedical Materials Research*, **59**, 585-590. https://doi.org/10.1002/jbm.1270

[30] Rodríguez-Vázquez, M., Vega-Ruiz, B., Ramos-Zúñiga, R., Saldaña-Koppel, D.A. and Quiñones-Olvera, L.F. (2015) Chitosan and Its Potential Use as a Scaffold for Tissue Engineering in Regenerative Medicine. *BioMed Research International*, **2015**, Article ID: 821279. https://doi.org/10.1155/2015/821279

[31] Spiller, K.L., Anfang, R.R., Spiller, K.J., Ng, J., Nakazawa, K., Daulton, J.W. and Vunjak-Novkovic, G. (2014) The Role of Macrophage Phenotype in Vascularization of Tissue Engineering Scaffolds. *Biomaterials*, **35**, 4477-4488. https://doi.org/10.1016/j.biomaterials.2014.02.012

[32] Li, P., Ohtsuki, C., Kokubo, T., Nakanishi, K., Soga, N., Nakamura, T. and Yamamuron, T. (1993) Effects of Ions in Aqueous Media on Hydroxyapatite Induction by Silica Gel and Its Relevance to Bioactivity on Bioactive Glass and Glass-Ceramics. *Journal of Biomaterials Applications*, **4**, 221-229. https://doi.org/10.1002/jab.770040303

[33] Nagai, N., Tsuji, T., Mohori, Y., Akagi, T. and Missana, L. (1990) Principles of Biomaterials and Tissue Responces. Part One: Osteogenic Cell Responces to Hydroxyapatite. *The International Journal of Oral & Maxillofacial Implants*, **3**, 423.